

## PAPER

# Quantitative Attractor Analysis of High-Capacity Kernel Logistic Regression Hopfield Networks

Akira TAMAMORI<sup>†</sup>, *Member*

**SUMMARY** Traditional Hopfield networks, trained with Hebbian learning, suffer from severe storage capacity limitations ( $P/N \approx 0.14$ ) and are prone to spurious attractors. Overcoming these issues is crucial for practical associative memory applications. While linear methods offer limited improvement, non-linear kernel methods, such as Kernel Logistic Regression (KLR), provide a powerful approach by mapping patterns to high-dimensional feature spaces, enhancing separability. Our previous work demonstrated KLR's capability to dramatically improve Hopfield network performance, achieving significantly higher storage capacity and noise robustness compared to Hebbian and linear logistic regression. Building on this, we perform a comprehensive quantitative analysis of the attractor structures in KLR-trained networks to understand the mechanisms behind these gains. Through extensive simulations, we systematically evaluated recall behavior from diverse initial states across wide ranges of storage loads ( $P/N$  up to 4.0) and initial noise levels. We quantified convergence to target patterns, other learned patterns, and spurious fixed points, and analyzed convergence speed. Our analysis confirms KLR's superior performance: the network achieves high storage capacity (up to  $P/N = 4.0$  demonstrated) and robustness, with near-perfect recall for low-noise inputs even at high loads. The attractor landscape is remarkably "clean", exhibiting near-zero rates of spurious fixed points across all tested conditions. We found that recall failures under high load and noise are primarily due to convergence to other learned patterns, not spurious ones. Recall dynamics are also exceptionally fast, typically within 1-2 steps for high-similarity states. This quantitative characterization of the attractor landscape provides crucial insights into how KLR reshapes network dynamics for high-capacity associative memory, establishing its effectiveness as a powerful training method and contributing to the understanding of high-performance associative memories.

**key words:** Hopfield network, Kernel logistic regression, Associative memory, Storage capacity, Noise robustness, Attractor analysis.

## 1. Introduction

Associative memory (AM) is a fundamental cognitive function that allows the retrieval of stored information based on partial or noisy cues. Artificial neural networks, particularly the Hopfield network [1], have served as foundational models for AMs due to their biologically plausible recurrent dynamics and the interpretation of stored memories as stable states (attractors) of an energy function. The recall process in a Hopfield network can be viewed as the network's state evolving towards a local minimum of its energy function, corresponding to the stored pattern most similar to the input cue.

Despite their conceptual elegance and biological inspiration, traditional Hopfield networks, primarily trained with the Hebbian learning rule [1], suffer from significant limi-

tations. A major challenge is their severely limited storage capacity, theoretically bounded around a pattern-to-neuron ratio ( $P/N$ ) of approximately 0.14 [2]. Exceeding this limit leads to catastrophic forgetting, retrieval errors, and the proliferation of spurious attractors – states that are not among the learned patterns but become stable fixed points of the network dynamics [3]. These spurious attractors interfere with proper recall and shrink the basins of attraction of the desired memories, severely impairing noise robustness.

To overcome these limitations, various methods have been proposed, often framing memory learning as a supervised task where the network's dynamics are shaped to make stored patterns stable fixed points. Linear approaches, such as those based on the pseudoinverse rule [4] or Linear Logistic Regression (LLR) [5], have shown moderate improvements in capacity and robustness. However, their effectiveness is fundamentally constrained by the requirement of linear separability of patterns in the input space, or within the neuron's input-output mapping.

The use of non-linear methods, particularly kernel methods, offers a promising avenue to transcend these limitations. Kernel methods, like Support Vector Machines (SVMs) or Kernel Ridge Regression (KRR) and Kernel Logistic Regression (KLR), implicitly map data into high-dimensional or infinite-dimensional feature spaces where complex non-linear relationships in the input space can become linearly separable [6]. Applying this powerful technique to the learning process of associative memories holds the potential for dramatically increased storage capacity and enhanced noise robustness.

Indeed, our previous work [7] demonstrated that Kernel Logistic Regression (KLR) learning can dramatically enhance the storage capacity and noise robustness of Hopfield networks. We showed that KLR, unlike linear methods, leverages kernels to implicitly map patterns to a high-dimensional feature space, achieving perfect recall even when pattern numbers exceeded neuron numbers (up to a ratio of 1.5 shown) and significantly enhancing noise robustness compared to Hebbian and LLR approaches.

While these results highlight the remarkable performance gains achievable with KLR, a detailed quantitative understanding of the attractor structures – the size and shape of the basins of attraction, the distribution and nature of spurious attractors, and the convergence dynamics – that are formed by KLR learning remains largely unexplored. Understanding how KLR reshapes the dynamical system of a Hopfield network to create such high-performance associative

Manuscript received January 1, 2015.

Manuscript revised January 1, 2015.

<sup>†</sup>The author is with the Department the Computer Science, Aichi Institute of Technology, Aichi, 470-0392, Japan.

DOI: 10.1587/transinf.E0.D.1

memory requires a comprehensive analysis of its attractor landscape.

In this paper, we present a comprehensive quantitative analysis of the attractor landscape in Hopfield networks trained using Kernel Logistic Regression. Leveraging extensive simulations on large networks ( $N = 500$ ), we systematically evaluate the network's recall performance and characterize its attractor structures across a wide range of storage loads ( $P/N$  up to 4.0) and initial noise levels.

The main contributions of this work are as follows:

1. We experimentally demonstrate that KLR-trained Hopfield networks achieve significantly higher storage capacity (up to  $P/N = 4.0$  demonstrated) and noise robustness compared to conventional methods.
2. We provide a detailed quantitative characterization of the attractor landscape, showing that KLR learning leads to a remarkably "clean" structure with near-zero rates of spurious fixed points across all tested conditions, even at high loads.
3. We reveal that the primary factor limiting recall performance under high load and high noise is not spurious attractor convergence, but rather the increased probability of converging to other learned patterns instead of the target, a key mechanism behind the noise robustness limit.
4. We show that the recall dynamics in KLR networks are extremely fast, typically converging within 1-2 steps for high-similarity initial states.

These findings offer deep insights into how kernel-based learning, specifically KLR, reshapes the dynamical system of a Hopfield network to create a highly effective associative memory, establishing KLR as a powerful and promising training method for such models and shedding light on the properties of high-capacity AMs.

## 2. Related Work

Traditional approaches to Hopfield network learning, primarily relying on Hebbian rules, suffer from limited storage capacity [1, 2] and the emergence of spurious attractors [3]. Linear learning methods, such as the pseudoinverse rule [4] and those based on Linear Logistic Regression (LLR) [5], offer some improvement but are fundamentally limited by the linear separability requirement of patterns in the input space.

The application of non-linear kernel methods to associative memory learning represents a promising direction. Kernel Associative Memories (KAM) [8] have been proposed, suggesting the theoretical possibility of unbounded capacity by leveraging high-dimensional feature spaces. Caputo and Niemann [9] provided an early theoretical analysis of KAM's storage capacity using spin glass theory for polynomial and Gaussian kernels, demonstrating increased capacity compared to the standard Hopfield model.

Building upon these foundations, our previous work [7] introduced and evaluated the use of Kernel Logistic Regres-

sion (KLR) for training Hopfield networks. We framed the learning task as a set of independent binary classification problems for each neuron, where KLR learns non-linear decision boundaries in a kernel-induced feature space. Our experiments demonstrated significant empirical gains: KLR dramatically improved storage capacity, achieving perfect recall even when the number of patterns exceeded neuron numbers (up to a ratio of 1.5 shown), and enhanced noise robustness, clearly outperforming both Hebbian and LLR approaches.

The present work is a direct continuation of [7], aiming to provide a detailed quantitative analysis of the attractor structures that lead to the high performance observed in KLR-trained networks. While [7] demonstrated that KLR achieves high capacity and robustness, this paper investigates how it does so by characterizing the resulting attractor landscape in detail. Other kernel-based approaches for associative memory include those based on Kernel SVM or Kernel Ridge Regression, often analyzed in the context of pattern classification or specific memory tasks rather than a full characterization of the Hopfield-like attractor dynamics [10].

## 3. Model and Methods

### 3.1 Network Model

We consider a standard Hopfield network composed of  $N$  fully-connected bipolar neurons, with states  $s_i \in \{-1, 1\}$  for  $i = 1, \dots, N$ . The network evolves over discrete time steps. Given a state  $s(t)$  at time  $t$ , the state  $s(t+1)$  at time  $t+1$  is determined by the activation of each neuron.

### 3.2 Learning Algorithms for Comparison

For comparison, we briefly describe the conventional Hebbian learning rule and Linear Logistic Regression (LLR) as implemented in our previous work [7].

#### 3.2.1 Hebbian Learning

The Hebbian learning rule sets the synaptic weights  $W_{ij}$  based on the correlation between the states of neurons  $i$  and  $j$  across  $P$  stored patterns  $\{\xi^\mu\}_{\mu=1}^P$ :

$$W_{ij} = \frac{1}{N} \sum_{\mu=1}^P \xi_i^\mu \xi_j^\mu \quad (i \neq j), \quad W_{ii} = 0$$

Recall is performed using the standard linear threshold dynamics:  $s_i(t+1) = \text{sign}\left(\sum_{j \neq i} W_{ij} s_j(t)\right)$ .

#### 3.2.2 Linear Logistic Regression (LLR)

In the LLR approach [5], learning for each neuron  $i$  is framed as predicting  $\xi_i^\mu$  from the states of other neurons  $\xi_{j \neq i}^\mu$ . A linear logistic regression model is trained for each neuron to

learn a weight vector  $w_i$ . The logit for neuron  $i$  given state  $s$  is  $h_i(s) = \sum_{j \neq i} w_{ij} s_j$ . The weights are learned by minimizing a regularized negative log-likelihood via gradient descent. The resulting  $N \times N$  symmetric weight matrix  $W_{ij}$  is used for recall with the same dynamics as Hebbian learning. More details on the LLR implementation can be found in [7].

### 3.3 Kernel Logistic Regression (KLR) Hopfield Network

The primary focus of this work is the Hopfield network trained using Kernel Logistic Regression, as detailed in our previous work [7]. KLR treats the learning for each neuron  $i$  as a binary classification task, predicting the target state  $t_i^\mu = (\xi_i^\mu + 1)/2 \in \{0, 1\}$  from the pattern  $\xi^\mu \in \{-1, 1\}^N$ .

KLR leverages the kernel trick [6] to implicitly map patterns into a high-dimensional feature space. The logit for neuron  $i$  given a pattern  $\xi$  is computed as a weighted sum of kernel similarities to the stored patterns:

$$h_i(\xi) = \sum_{\mu=1}^P \alpha_{\mu i} K(\xi, \xi^\mu)$$

We employ the Radial Basis Function (RBF) kernel  $K(x, y) = \exp(-\gamma \|x - y\|^2)$ , which measures the similarity between patterns in the feature space.

The dual variables  $\alpha_i = [\alpha_{1i}, \dots, \alpha_{Pi}]^T$  for each neuron  $i$  are learned by minimizing the L2-regularized negative log-likelihood objective using gradient descent. The learning parameters were set based on empirical findings in [7] to achieve robust performance: number of updates = 200, learning rate = 0.1, and L2 regularization parameter  $\lambda = 0.01$ . The RBF kernel parameter was set to  $\gamma = 1/N$ .

### 3.4 Recall Process

The recall process in KLR-trained networks differs from Hebbian/LLR as it does not rely on an explicit  $N \times N$  weight matrix. Given a network state  $s(t)$  at time  $t$ , the next state  $s(t+1)$  is determined by the sign of the activation potential for each neuron, relative to a threshold  $\theta$ :

$$s_i(t+1) = \text{sign}(h_i(s(t)) - \theta_i)$$

where  $h_i(s(t)) = \sum_{\mu=1}^P \alpha_{\mu i} K(s(t), \xi^\mu)$  is the logit for neuron  $i$ . In this work, the threshold vector was set to  $\theta = \mathbf{0}$ , meaning  $\theta_i = 0$  for all  $i$ . The recall process involves computing kernel values between the current state and all  $P$  stored patterns at each step.

### 3.5 Experimental Setup

We conducted extensive simulations on networks with  $N = 500$  neurons to quantitatively analyze the attractor landscape. Stored patterns were generated as random bipolar vectors  $\{-1, 1\}^N$ , with each element chosen independently with equal probability. The number of stored patterns,  $P$ , was varied to achieve different storage loads, defined by the

ratio  $P/N$ . We evaluated  $P/N$  ratios ranging from 0.05 to 4.0.

The KLR learning parameters were set as described in Section 3.3.

### 3.6 Attractor Structure Analysis Methodology

To characterize the attractor landscape, we performed systematic recall simulations from various initial states and analyzed their convergence behavior. For each combination of parameters ( $P/N$  ratio and initial noise level), we conducted multiple recall trials.

#### 3.6.1 Initial State Generation

For a given  $P/N$  ratio,  $P$  random patterns were generated and learned. For each learned pattern, we generated multiple initial states by introducing controlled noise. Noise was introduced by flipping a fraction of bits in the target pattern to achieve a specific initial similarity, measured by the direction cosine between the initial state  $s(0)$  and the target pattern  $\xi^\nu$ . The initial similarity was varied across a range of values (e.g., 0.05 to 1.0). For each learned pattern and each initial similarity level, we generated 5 distinct initial states. The total number of recall trials for a given  $P/N$  ratio and initial similarity level was  $P \times 5$ .

#### 3.6.2 Recall Simulation and Convergence

Each initial state was used as the starting point for the recall dynamics, which was simulated for a maximum of 30 discrete time steps. Convergence was detected when the network state remained unchanged for one consecutive step (indicating a fixed point). Trials that did not reach a fixed point within 30 steps were classified as not converged (although in our experiments, all trials converged to fixed points).

#### 3.6.3 Convergence Destination Classification

The final state  $s_{\text{final}}$  reached by each recall trial was classified into one of the following categories:

**Target Pattern:**  $s_{\text{final}}$  is identical to the original target pattern  $\xi^\nu$  from which the initial state was generated.

**Other Learned Pattern:**  $s_{\text{final}}$  is identical to one of the other  $P - 1$  learned patterns  $\xi^\mu$  ( $\mu \neq \nu$ ).

**Spurious Fixed Point:**  $s_{\text{final}}$  is a fixed point but is not identical to any of the  $P$  learned patterns.

**Not Converged / Cycle:** The trial did not reach a fixed point within the maximum number of steps. (Note: In our experiments, all trials converged to fixed points).

Identity was strictly checked using array equality for bipolar  $\{-1, 1\}$  vectors.

#### 3.6.4 Quantitative Metrics

Based on the classification of recall trials, we computed the

following quantitative metrics to characterize the attractor landscape:

**Fixed Point Rate:** The proportion of trials that converged to any fixed point (including target, other learned, and spurious).

**Not Converged Rate:** The proportion of trials that did not converge to a fixed point within the maximum steps.

**Target Recall Rate:** The proportion of trials that converged specifically to the target pattern. This metric quantifies the size of the target pattern’s basin of attraction for a given initial noise level.

**Other Learned Recall Rate:** The proportion of trials that converged to one of the other learned patterns.

**Spurious Fixed Point Rate:** The proportion of trials that converged to a spurious fixed point.

**Average Final Direction Cosine to Target:** The average direction cosine between the final state and the target pattern, averaged over all trials for a given initial similarity level.

**Average Steps to Converge:** The average number of steps taken to reach a fixed point, averaged over all trials that converged to a fixed point.

### 3.6.5 Random Seed Management

To ensure reproducibility of pattern generation and learning outcomes while allowing for diverse initial noise instantiations, we carefully managed random seeds. A fixed seed was used for generating the set of  $P$  patterns. A different fixed seed was used for the KLR learning process given these patterns. For generating the initial states for each trial, the random seed was varied (e.g., based on the loop indices or system time) to ensure different random bit flips were applied for each trial.

## 4. Results

We conducted extensive simulations to quantitatively analyze the attractor landscape of KLR-trained Hopfield networks. Networks with  $N = 500$  neurons were trained with various numbers of random bipolar patterns  $P$ , covering storage loads ( $P/N$ ) ranging from 0.05 to 4.0. For each storage load, recall dynamics were evaluated from initial states with varying degrees of noise, quantified by the initial similarity (direction cosine) ranging from 0.05 to 1.0. For each combination of  $P/N$  ratio and initial similarity, 5 recall trials were performed for each of the  $P$  learned patterns, and the convergence destination and speed were analyzed as described in Section 3.6.

### 4.1 Storage Capacity and Noise Robustness

Figure 1 shows the Target Recall Rate as a function of the storage load ( $P/N$ ) for different initial similarity levels. As observed in our previous work [7] and extended in this study,

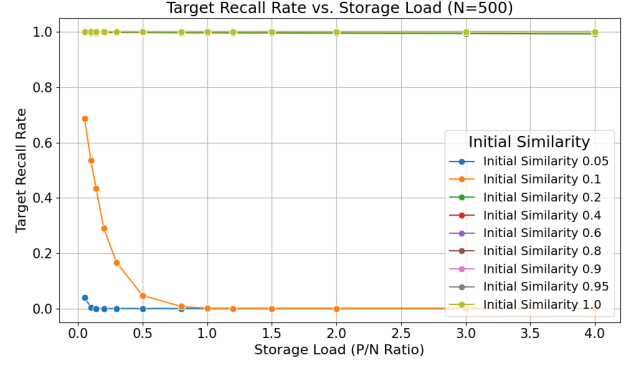


Fig. 1: Target Recall Rate vs. Storage Load ( $P/N$ ) for different Initial Similarity levels. The graph shows the proportion of trials that converged to the target pattern as a function of storage load. Different lines represent results for different initial similarity levels, indicating the network’s capacity under varying noise. Results are averaged over all learned patterns and recall trials for each parameter combination ( $N = 500$ ).

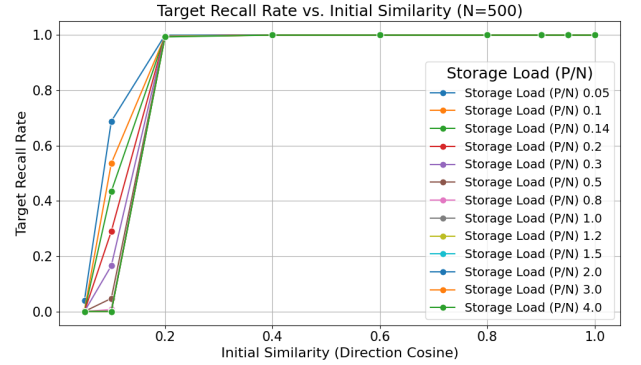


Fig. 2: Target Recall Rate vs. Initial Similarity. The graph shows the proportion of trials that converged to the target pattern as a function of the initial similarity (direction cosine), quantifying noise robustness. Different lines represent results for various storage loads ( $P/N$ ). Results are averaged over all learned patterns and recall trials for each parameter combination ( $N = 500$ ).

KLR-trained networks demonstrate significantly higher storage capacity compared to the Hebbian limit ( $\approx 0.14$ ) and LLR performance ( $\approx 0.85$ ). Notably, for initial similarity of 1.0 (no noise), the Target Recall Rate remains 1.0 across the entire tested range, up to  $P/N = 4.0$ . This indicates that KLR can store and perfectly recall a number of patterns significantly exceeding the number of neurons.

The graph also reveals that the storage capacity is highly dependent on the initial similarity (noise level). For high initial similarity (e.g., 0.8, 0.9, 1.0), the Target Recall Rate remains high even at large  $P/N$ . However, as initial similarity decreases (e.g., 0.4, 0.2, 0.1, 0.05), the Target Recall Rate begins to drop at lower  $P/N$  ratios. This indicates that the network’s capacity under noisy conditions is lower than its

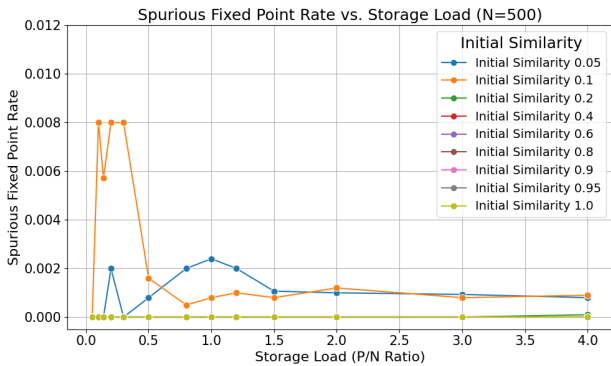


Fig. 3: Spurious Fixed Point Rate vs. Storage Load ( $P/N$ ) for different Initial Similarity levels. The graph shows the proportion of trials that converged to a spurious fixed point as a function of storage load. Different lines represent results for varying initial similarity, illustrating the rate of emergence of unintended fixed points. Results are averaged over all learned patterns and recall trials for each parameter combination ( $N = 500$ ).

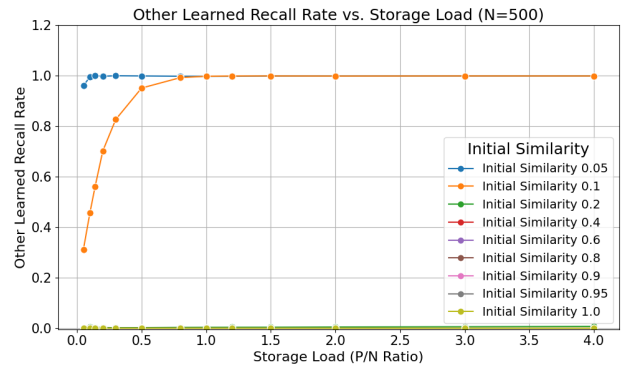


Fig. 4: Other Learned Recall Rate vs. Storage Load ( $P/N$ ) for different Initial Similarity levels. The graph shows the proportion of trials that converged to a different learned pattern (not the target) as a function of storage load. Different lines represent results for varying initial similarity, indicating mis-recall to other stored memories. Results are averaged over all learned patterns and recall trials for each parameter combination ( $N = 500$ ).

theoretical capacity with perfect cues. For an initial similarity of 0.2, the Target Recall Rate begins to drop significantly around  $P/N = 1.5$  and reaches near zero by  $P/N = 4.0$ . For very low initial similarity (0.05, 0.1), the Target Recall Rate is low even at low loads and drops rapidly.

Figure 2 complements these results by showing the Target Recall Rate as a function of initial similarity for different storage loads. This graph clearly illustrates the network’s noise robustness. At low storage loads (e.g.,  $P/N = 0.05, 0.1$ ), near-perfect recall is achieved even from highly noisy initial states (low initial similarity). As storage load increases, the noise robustness decreases, indicated by the shift of the curves to the right; higher initial similarity is required to achieve high recall rates at higher  $P/N$ .

#### 4.2 Attractor Landscape Analysis

To understand the high performance of KLR networks, we characterized the structure of the resulting attractor landscape by classifying the convergence destination of each recall trial. Figure 3 shows the Spurious Fixed Point Rate as a function of storage load for different initial similarity levels. Strikingly, the rate of convergence to spurious fixed points is near zero across all tested  $P/N$  ratios (up to 4.0) and initial similarity levels. This is a significant finding, as spurious attractors are a major limitation in traditional Hopfield networks.

Figure 4 shows the Other Learned Recall Rate as a function of storage load. Similar to the spurious rate, the Other Learned Recall Rate is low when initial similarity is high. However, for low initial similarity (e.g., 0.05, 0.1, 0.2), the Other Learned Recall Rate increases significantly as storage load increases, particularly beyond  $P/N \approx 0.8$ .

Figure 5 combines these results, illustrating the decomposition of recall failures ( $1.0 - \text{Target Recall Rate}$ , for cases

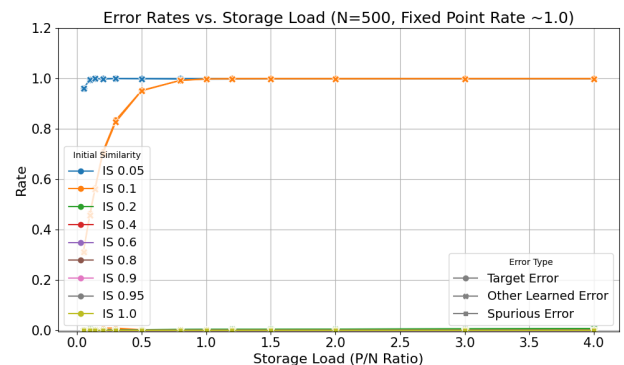


Fig. 5: Decomposition of Error Rates vs. Storage Load ( $P/N$ ) for different Initial Similarity levels. The graph shows how the total error rate ( $1.0 - \text{Target Recall Rate}$ , assuming Fixed Point Rate  $\approx 1.0$ ) is composed of failures to converge to the target pattern. Lines show the Target Error ( $1.0 - \text{Target Recall Rate}$ ), Other Learned Error (convergence to other learned patterns), and Spurious Error (convergence to spurious fixed points), decomposed by error type and initial similarity (IS). Results are averaged over all learned patterns and recall trials for each parameter combination ( $N = 500$ ).

where Fixed Point Rate is near 1.0) into convergence to Other Learned Patterns and Spurious Fixed Points. This graph clearly shows that for initial similarity levels below approximately 0.8, the primary component of recall failure at higher storage loads is convergence to other learned patterns, rather than spurious ones. This is a key mechanism limiting noise robustness at high capacity. The Spurious Error remains remarkably low across all conditions.

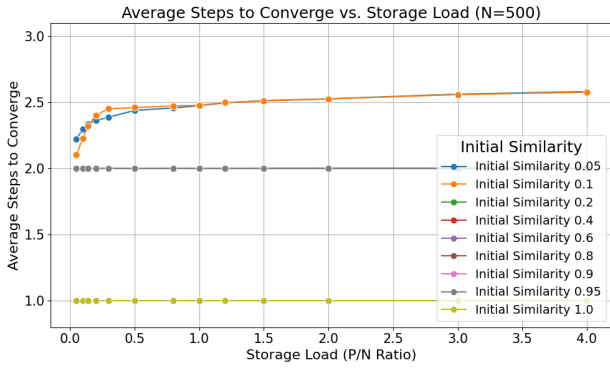


Fig. 6: Average Steps to Converge vs. Storage Load ( $P/N$ ) for different Initial Similarity levels. The graph shows the average number of discrete time steps required for trials that converged to a fixed point. Different lines represent results for varying initial similarity, illustrating the speed of the recall dynamics. Results are averaged over all learned patterns and convergent recall trials for each parameter combination ( $N = 500$ ).

### 4.3 Recall Dynamics

Figure 6 presents the Average Steps to Converge as a function of storage load. For initial similarity of 1.0 (perfect cue), the network converges in a single step, as expected for a learned pattern. For noisy initial states, the convergence is also extremely fast, typically occurring within 2 steps for initial similarity down to approximately 0.2. For very low initial similarity (0.05, 0.1), the average steps to converge are slightly higher (around 2.3-2.5 steps) when convergence to learned patterns occurs, but still well within the maximum simulation steps (30). This indicates that KLR networks exhibit very fast recall dynamics, reaching stable states quickly.

Figure 7 shows the Average Final Direction Cosine to the Target Pattern as a function of storage load for different initial similarity levels. This metric provides a continuous measure of recall quality. For high initial similarity, the average final direction cosine is very close to 1.0, confirming near-perfect recall. As storage load increases or initial similarity decreases, the average final direction cosine decreases. For conditions where Target Recall Rate is low (e.g., low initial similarity at high  $P/N$ ), the average final direction cosine remains positive but significantly less than 1.0. This indicates that while the network doesn't converge exactly to the target pattern, the final states are still more similar to the target than to random states (which would have a direction cosine around 0), reflecting convergence to other learned patterns or nearby spurious states.

## 5. Discussion

Our extensive quantitative analysis of the attractor landscape in KLR-trained Hopfield networks reveals key mechanisms underlying their exceptionally high storage capacity

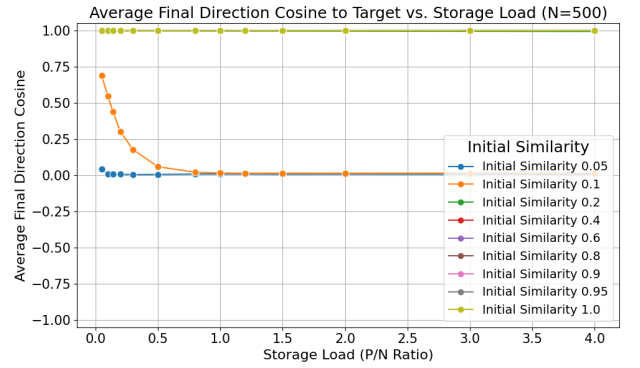


Fig. 7: Average Final Direction Cosine to Target vs. Storage Load ( $P/N$ ) for different Initial Similarity levels. The graph shows the average direction cosine between the final state and the target pattern across all trials. Different lines represent results for varying initial similarity. A value of 1.0 indicates perfect recall, while values close to -1.0 indicate convergence to the inverted pattern (not expected for KLR) or a spurious state far from the target. Results are averaged over all learned patterns and recall trials for each parameter combination ( $N = 500$ ).

and noise robustness, significantly exceeding the limitations of traditional Hebbian learning and linear approaches like LLR. The detailed characterization of attractor structures provides novel insights into how kernel-based learning reshapes the dynamical system of associative memory.

The most striking finding is the demonstration of KLR's ability to achieve and maintain near-perfect recall for storage loads up to  $P/N = 4.0$  for low-noise initial states. This vastly surpasses the classical Hebbian capacity limit of  $\approx 0.14$  and significantly exceeds typical LLR performance ( $\approx 0.85$ ). This empirical result strongly supports the theoretical potential for increased capacity suggested by earlier work on Kernel Associative Memories (KAM) [8, 9], demonstrating that KLR, as a practical learning algorithm, can effectively leverage this potential in finite-sized networks.

Our attractor analysis provides a clear explanation for these performance gains. KLR learning leads to a remarkably "clean" attractor landscape, characterized by near-zero rates of spurious fixed points across all tested conditions, even at high storage loads where traditional methods would exhibit a proliferation of such unwanted attractors [3]. This dramatic suppression of spurious attractors ensures that recall dynamics primarily converge towards desired memories.

Furthermore, the high Target Recall Rate, particularly at lower storage loads and moderate noise levels, indicates that KLR creates large basins of attraction around the learned patterns. This enhanced basin size directly contributes to the network's superior noise robustness compared to Hebbian and LLR (as shown in Figure 2), allowing retrieval from significantly corrupted initial states.

While KLR demonstrates remarkable capacity and robustness, our analysis of error rates under high load and high noise reveals the primary mechanism limiting performance

in these challenging regimes. Figure 5 clearly shows that recall failures (1.0 - Target Recall Rate) are predominantly due to convergence to other learned patterns, rather than spurious ones. As initial noise increases and storage load grows, the probability of being drawn to a different, albeit learned, attractor increases, competing with convergence to the intended target pattern. This "mis-recall" to other learned memories, rather than convergence to non-learned spurious states, appears to be the main factor defining the boundary of the basin of attraction for the target pattern under noisy, high-load conditions. This contrasts with Hebbian networks, where spurious attractors are the dominant cause of failure near capacity.

Note that in this study, a fixed point is defined as spurious only if it does not match any of the  $P$  learned patterns. Thus, convergence to a non-target but learned pattern is not classified as spurious, although it still constitutes a recall error. Our analysis distinguishes between convergence to other learned patterns and convergence to spurious fixed points, highlighting that in KLR, the former is the dominant form of recall error at high loads and noise.

The observed recall dynamics are also notably fast, typically converging within 1-2 steps for initial states with high similarity (Figure 6). Even for lower similarity, convergence to fixed points generally occurs within a few steps. This rapid convergence is advantageous for practical applications requiring quick retrieval.

Delving into the mechanisms behind the clean attractor landscape, particularly the dramatic suppression of spurious fixed points, several factors related to KLR and kernel methods are likely at play. KLR operates by implicitly mapping patterns into a high-dimensional feature space [6] where, ideally, they become linearly separable according to the target labels for each neuron. The KLR learning objective (minimizing regularized logistic loss) aims to find a decision boundary in this feature space that achieves optimal separation. We hypothesize that this process of finding a "clean" separation in the feature space translates into a corresponding "clean" separation of attractor basins in the input space, effectively pushing potential spurious minima away from regions that would attract recall trajectories. In contrast, Hebbian learning, based on simple correlation, is known to create complex energy landscapes with many local minima (spurious attractors) even for relatively simple pattern sets [3]. Linear methods, constrained by the input space or fixed linear feature mapping, are less capable of achieving the intricate, non-linear separation needed to suppress spurious states arising from densely packed or correlated patterns at higher loads. The regularization term ( $\lambda\|\alpha\|^2$ ) in the KLR objective may also play a role in shaping the feature space representation or the smoothness of the implicit decision boundary, potentially contributing to a less complex energy landscape with fewer spurious minima, although its primary effect is typically on preventing overfitting.

The ability of KLR to create such a favorable attractor landscape is likely attributable to its use of kernel methods. By implicitly mapping patterns into a high-dimensional fea-

ture space (as discussed in Section 3.3 and [6]), KLR can potentially achieve linear separability of patterns that are not separable in the original input space. The learning objective of KLR (minimizing regularized logistic loss) then effectively finds a decision boundary in this feature space that separates patterns according to their target values. This separation in the feature space seems to translate into well-defined, widely separated basins of attraction for learned patterns in the input space, while simultaneously inhibiting the formation of spurious minima.

Our findings align with and extend the theoretical framework of KAM [8, 9] by providing concrete empirical evidence for the high performance and specific attractor properties achieved by a practical kernel-based learning algorithm. Kernel Ridge Regression (KRR) [10] represents another prominent kernel-based approach for supervised learning that could be applied to associative memory. Like KLR, KRR also leverages the kernel trick to map data into a feature space. However, instead of minimizing logistic loss for classification, KRR minimizes squared error loss for regression, aiming to predict continuous target values (e.g., +1/-1 states). A key difference is that standard KRR has a non-iterative, closed-form solution for the optimal dual variables, making its learning process significantly faster than KLR's iterative gradient descent, particularly for large numbers of patterns. Although both KLR and KRR share the same kernel-based framework, their differing loss functions (logistic vs. squared error) and learning algorithms may lead to distinct attractor landscape characteristics and performance trade-offs. A detailed comparison of the attractor structures and performance trade-offs between KLR and KRR would be a valuable future direction.

However, the computational cost of recall in KLR networks, which involves computing kernel values between the current state and all  $P$  stored patterns at each step ( $O(NP)$  complexity), remains a practical consideration, especially at very high storage loads ( $P \gg N$ ). This contrasts with the  $O(N^2)$  complexity of recall in Hebbian or LLR networks. Future work should explore efficient kernel approximation methods [11] to mitigate this scalability challenge for large-scale applications.

Further research directions include investigating the impact of different kernel types and hyperparameters on attractor structures, developing online or incremental kernel learning algorithms, and exploring the application of KLR-trained networks to more complex, structured data and tasks. A deeper theoretical analysis using tools from dynamical systems theory or statistical mechanics, perhaps building upon the KAM Hamiltonian framework [9] or Koopman operator theory, could provide further analytical insights into the observed attractor properties and capacity limits.

## 6. Conclusion

In this paper, we presented a comprehensive quantitative analysis of the attractor landscape in Hopfield networks trained with Kernel Logistic Regression (KLR), aiming

to elucidate the mechanisms behind its previously demonstrated high storage capacity and noise robustness. Through extensive simulations on large networks, we systematically characterized the network's recall behavior and attractor structures across a wide range of storage loads and initial noise levels.

Our findings confirm that KLR provides a powerful learning mechanism for associative memory, dramatically surpassing the storage capacity limitations of traditional Hebbian learning and linear approaches. We empirically demonstrated high storage capacity, with near-perfect recall achievable up to  $P/N = 4.0$  for low-noise conditions, and significant noise robustness.

The detailed quantitative analysis of the attractor landscape revealed a remarkably "clean" structure, characterized by near-zero rates of spurious fixed points across all tested conditions. This suppression of spurious attractors contributes significantly to KLR's high performance. Furthermore, we identified that the primary factor limiting recall performance under high load and noise is the increased tendency to converge to other learned patterns, rather than spurious ones.

We also showed that the recall dynamics in KLR networks are exceptionally fast, typically resulting in convergence within 1-2 steps for high-similarity initial states.

In summary, our work provides crucial empirical evidence and quantitative characterization of the attractor landscape properties that enable KLR-trained Hopfield networks to function as high-capacity and robust associative memories. By effectively leveraging kernel methods to reshape the network's dynamics and attractor structures, KLR overcomes the long-standing limitations of Hopfield networks.

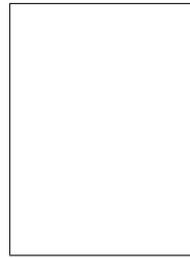
While acknowledging the practical consideration of computational cost during recall at very high storage loads, the demonstrated significant performance gains in both capacity and robustness establish KLR as a potent method for enhancing the capabilities of Hopfield-like associative memory systems. Future work will explore computational efficiency improvements, alternative kernel-based approaches like KRR, and deeper theoretical analysis of the observed attractor properties. This research highlights the potential of applying modern machine learning techniques to advance our understanding and capabilities in associative memory.

## References

- [1] J.J. Hopfield, "Neural networks and physical systems with emergent collective computational abilities.," Proceedings of the National Academy of Sciences, vol.79, no.8, pp.2554–2558, 1982.
- [2] D.J. Amit, H. Gutfreund, and H. Sompolinsky, "Storing infinite numbers of patterns in a spin-glass model of neural networks," Phys. Rev. Lett., vol.55, pp.1530–1533, Sep 1985.
- [3] D.J. Amit, H. Gutfreund, and H. Sompolinsky, "Spin-glass models of neural networks," Phys. Rev. A, vol.32, pp.1007–1018, Aug 1985.
- [4] T. Kohonen, Self-organization and associative memory: 3rd edition, Springer-Verlag, Berlin, Heidelberg, 1989.
- [5] D.J.C. MacKay, Information Theory, Inference & Learning Algorithms, Cambridge University Press, USA, 2002.
- [6] B. Scholkopf and A.J. Smola, Learning with Kernels: Support Vector

Machines, Regularization, Optimization, and Beyond, MIT Press, Cambridge, MA, USA, 2001.

- [7] A. Tamamori, "Kernel logistic regression learning for high-capacity hopfield networks," arXiv:2504.07633, 2025.
- [8] D. Nowicki and H. Siegelmann, "Flexible kernel memory," PLOS ONE, vol.5, no.6, pp.1–18, 06 2010.
- [9] B. Caputo and H. Niemann, "Storage capacity of kernel associative memories," Proceedings of the International Conference on Artificial Neural Networks, ICANN '02, Berlin, Heidelberg, p.51–56, Springer-Verlag, 2002.
- [10] A. Tamamori, "Kernel ridge regression for efficient learning of high-capacity hopfield networks," arXiv:2504.12561, 2025.
- [11] C.K.I. Williams and M. Seeger, "Using the nystrom method to speed up kernel machines," Advances in Neural Information Processing Systems, 2000.



**Akira Tamamori** He received his B.E., M.E., and D.E. degrees from Nagoya Institute of Technology, Nagoya, Japan, in 2008, 2010, 2014, respectively. From 2014 to 2016, he was a Research Assistant Professor at Institute of Statistical Mathematics, Tokyo, Japan. From 2016 to 2018, he was a Designated Assistant Professor at the Institute of Innovation for Future Society, Nagoya University, Japan. From 2018 to 2020, he was an lecturer at Aichi Institute of Technology, Japan. He has been an Associate Professor at the same institute. He is also a Visiting Assistant Professor at Speech and Language Processing Laboratory, Japan. His research interests include speech signal processing, and machine learning. He is a member of the Institute of Electronics, Information and Communication Engineers (IEICE), the Acoustical Society of Japan (ASJ), International Speech Communication Association (ISCA), and Asia-Pacific Signal and Information Processing Association (APSIPA).